International Journal of Innovative
Computing, Information and Control
Volume **8**, Number **9**, September **2012**

 ISSN 1349-4198
pp. 6461–6471

BOVINE IRIS SEGMENTATION USING REGION-BASED ACTIVE CONTOUR MODEL

Shengnan Sun and Lindu Zhao*

Institute of Systems Engineering
Southeast University
No. 2, Sipailou, Nanjing 210096, P. R. China
shengnansun1984@gmail.com; *Corresponding author: ldzhao@seu.edu.cn

Received May 2011; revised October 2011

Abstract. *Iris recognition is one of the most reliable and accurate biometric technologies, as the richness and apparent stability of the iris texture make it robust. Iris segmentation is a critical part in iris recognition, because it defines the inner and outer boundaries of iris region which is used for feature analysis. Active contour model, also known as snake, is a powerful image segmentation technique. This paper proposes a novel global and local region-based active contour model to extract the bovine iris from the surrounding structures. The proposed active contour model elicits the iris texture in an iterative fashion and is guided by both global and local intensity information of the image. Then, iris region is normalized into rectangle shape, which is convenient for later feature extraction. Experimental result indicates the efficacy of the proposed technique.*
Keywords: Iris recognition, Iris segmentation, Active contour, Level sets, Partial differential equations

1. **Introduction.** The iris is an internal organ of the eye which is located behind the cornea and in front of the lens. Flome et al. [1] postulated that the textural content of the iris is stable throughout an individual's lifespan. They stated that every iris is unique and no two individuals have similar irises. Hence, iris recognition becomes an emerging identification technology based on biometrics with its low False Accept Rate (FAR). In the past twenty years, human iris recognition has developed rapidly, and the most mature technologies are introduced by Daugman [2] and Tan [3] respectively. Both of their iris recognition systems have been commercialized. Since 2001, iris recognition technology has also been applied in animal individual identification. Suzaki developed an animal iris recognition system for the horse race [4]. As food securities crises, such as BSE and hand-foot-and-mouth disease, posed a threat to human health, a tracking and traceability system using iris recognition was introduced to ensure food safety [5,35]. Iris segmentation (iris localization or iris edge detection), which aims to isolate the actual area from the eye image, plays a vital role in iris recognition. The following steps (involving normalization, enhancement, feature extraction and matching test, as shown in Figure 1) are based on the results of iris segmentation. And the final performance of iris recognition system is partly dependent on the accuracy of iris segmentation.

Because of the importance of iris segmentation, a number of algorithms have been developed to achieve accurate and fast iris localization. The integro-differential operator, which acts as a circle edge detector, is employed for determining the inner and outer boundaries of iris [6,7,15]. Wildes [8] applied Hough transform-based method to segmenting the iris, and the upper and lower boundaries of the eyelid are approximated using parabolic curves. Several other localization methods based on Hough-transform to segment the iris were introduced by Ma [9,10], Huang [11], Lim [12], and Yuan [13] respectively. Boles and Boashash [14] got the iris from the image by edge and contour detection. He et al. [16]

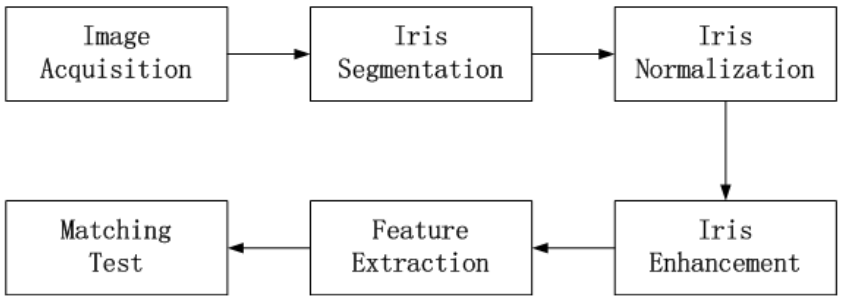

FIGURE 1. Iris recognition framework

proposed a novel iris localization method based on a spring force-driven iteration scheme, which was inspired by Hook's Law.

All above methods usually consider iris contour as circles or ellipses, while recently active contour has been utilized to improve the performance, which take iris contours as deformable boundaries and get the iris boundary without prior shape information. Abhyankar and Schuckers designed training based active shape model to segment the iris from the sclera [17]. In their model, nonlinear shape of the iris was learned using a few training images. Daugman introduced an excellent way to describe the iris inner and outer boundaries in terms of "active contour" [18]. Geodesic active contour was employed to extract the iris from the surrounding structures by Shah and Ross [19]. Roy, Bhattacharya et al. [20] introduced a region-based active contour model to segment the iris from unideal image. Zhang et al. [34] introduced an improved level set based active contour to segment the iris. In their method, local gradient extremes are removed before applying active contour method.

Since there are distinct differences between human and bovine irises, iris segmentation algorithms developed for human iris usually perform poorly while applied to bovine iris. Although Zhang et al. [36] introduced a two-step localization method to segment the bovine iris by combining threshold transform and Sobel edge detection, the out boundary of bovine iris is not highly precise, due to the intensity inhomogeneity. In this paper, we propose a novel iris segmentation method for bovine iris recognition, based on the active contour. The remainder of this paper is organized as follows. In Section 2, some well known existing active contour models are reviewed briefly. Section 3 provides the bovine iris segmentation method based on global and local region-based active contour model. And then, implementation and iris normalization are described detailedly in Section 4. Section 5 concludes the paper.

2. Active Contour Methods.

Active contours, the snake model originally introduced by Kass et al. [21], is a classical approach to edge detection based on deforming an initial contour towards the boundary of the object to be detected, and it is widely used in medical image processing [30,32,37] and iris recognition [18-20]. This model corresponds to an elastic curve that is propagated by image forces towards the minimum of an energy generated from an image. Generally speaking, the existing active contour models can be classified into two types: edge-based models and region-based models. Each of them has its own pros and cons.

2.1. Edge-based active contour model.

Generally, there are two types of edge-based active contour models in literature: parametric active contours [21] and geometric active contours [22-24]. And there exits an explicit mathematical equivalence relationship between the two active contours [25]. The edge-based active contour model utilizes image

gradient as an additional constraint to stop the contours on the boundaries of object. The classic edge-based active contour model is formulated by minimizing an energy functional that takes a minimum when contours are smooth and reside on object boundaries. Given a gray-level image $I(x, y)$ and a varying curve $C(s) = [x(s), y(s)],\ s \in [0, 1]$, the energy function is written as

$$E = \int_0^1 \frac{1}{2}\left[\alpha \left|C'(s)\right|^2 + \beta \left|C''(s)\right|^2\right] + E_{ext}(C(s))ds \tag{1}$$

The first term is the internal energy, which is sum of elastic and rigid forces. α and β are weighting parameters which control the snake's tension and rigidity respectively, and $C'(s)$ and $C''(s)$ denote the first and second derivatives of $C(s)$. The external energy function E_{ext} is derived from the image, which is designed to pull the active contour towards object boundaries or other features of interest. Typical external energies are

$$E_{ext}^{(1)}(x, y) = -\left|\nabla I(x, y)\right|^2 \tag{2}$$

$$E_{ext}^{2}(x, y) = -\left|\nabla [G_\sigma(x, y) * I(x, y)]\right|^2 \tag{3}$$

where $G_\sigma(x, y)$ is a two-dimension Gaussian function with standard deviation σ and ∇ is the gradient operator. A snake that minimizes E must satisfy the equation

$$F_{int} + F_{ext} = 0 \tag{4}$$

where $F_{int} = \alpha C''(s) - \beta C''''(s)$ and $F_{ext} = -\nabla E_{ext}$. The internal force F_{int} controls the smoothness of the contour while the external force F_{ext} pulls the snake toward the desired image edges.

All these edge-based active contours rely on the image gradient $|\nabla I(x, y)|$ to stop the curve evolution. If the image is very noisy or the gradients are discrete, the curve may pass through the desired boundary. Hence, it is important to design suitable external force while applying edge-based active contour to real images.

2.2. **Region-based active contour model.** As the edge-based active contours performed imperfectly for the weakness of stopping edge-function, Chan and Vese [26] proposed an active contour model (CV model) based on the Mumford-Shah model [27]. For an image $I(x, y)$ on the image domain Ω, they proposed to minimize the energy

$$E^{CV}(C, c_1, c_2) = \lambda_1 \int_{C_{in}} \left|I(x) - c_1\right|^2 dx + \lambda_2 \int_{C_{out}} \left|I(x) - c_2\right|^2 dx + \upsilon \left|C\right| \tag{5}$$

where $\upsilon \geq 0$, $\lambda_1, \lambda_2 > 0$ are fixed parameters. C_{in} and C_{out} represent the region inside and outside of the contour C (or object) respectively, and the parameters c_1 and c_2 are two constants that approximate the image intensity in domain C_{in} and C_{out}. Equation (5) is known as global binary fitting energy. This energy can be represented by a level set formulation, and then energy minimization problem can be converted to solving the level set evolution equation.

The CV model performs quite well while applied to homogeneous image. However, in practice, the image is inhomogeneous, whose intensity in either C_{in} or C_{out} is not constant. Therefore, it is difficult for CV model to get the accurate object contour from noisy images.

3. **Iris Segmentation.** Like human eye (Figure 2(a)), the image of cattle eye is composed of pupil, iris and sclera, as shown in Figure 2(b). Sometimes, lash and eyelid also may appear in the image. Obviously, the image intensities are inhomogeneous in pupil, iris and sclera parts, as noise exits.

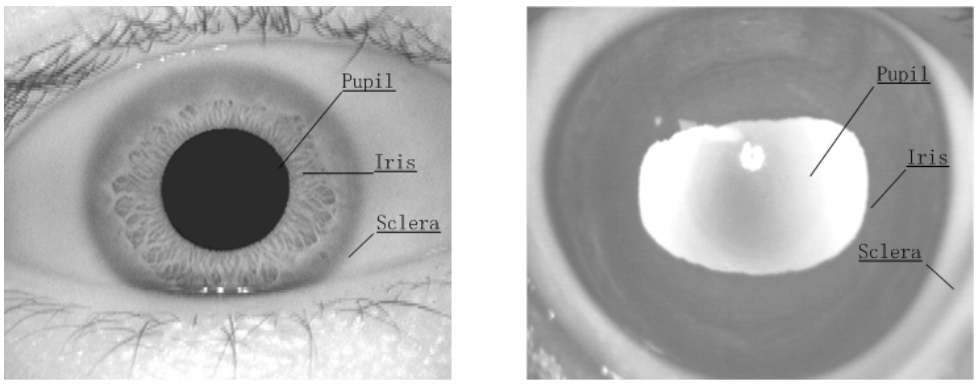

(a) (b)

FIGURE 2. (a) Human eye image and (b) cattle eye image

The aim of iris segmentation is to get the inner and outer boundaries of iris. There are obvious intensity differences among pupil, iris and sclera. And intensity inhomogeneity occurs in cattle eye image, due to technical limitations or artifacts introduced by the object being imaged.

3.1. **Global and local region-based active contour model.** In this subsection, we propose a global and local region-based framework using intensity information. The framework is composed by two parts, global and local parts. Consider a given vector valued image $I : \Omega \to \Re^d$, where $\Omega \subset \Re^n$ is the image domain, and d is the dimension of the vector. In particular, $d = 1$ is for gray level images, as $d = 3$ for color images. In this paper, the bovine eye image is treated as a gray level image.

We use x and y as independent spatial variables each representing a single point in Ω. Using this notation, we introduce a mask function in terms of a radius parameter r

$$M(x, y, r) = \begin{cases} 1, & \|x - y\| \le r \\ 0, & \text{otherwise} \end{cases} \tag{6}$$

where $M(x, y, r)$ is used to mask local region. This function will be equal to 1 when point y is within a ball of radius r centered at x, and 0 otherwise. As shown in Figure 3, let C be a closed contour in the image domain Ω, which separated Ω into two regions: $\Omega_1 = inside(C)$ and $\Omega_2 = outside(C)$. For a given point $x \in \Omega$, the local energy at point x is defined as:

$$E_x^{local}(C, f_1(x), f_2(x)) = \sum_{i=1}^{2} \lambda_i \int_{\Omega_i} M(x, y, r) \left| I(y) - f_i(x) \right|^2 dy \tag{7}$$

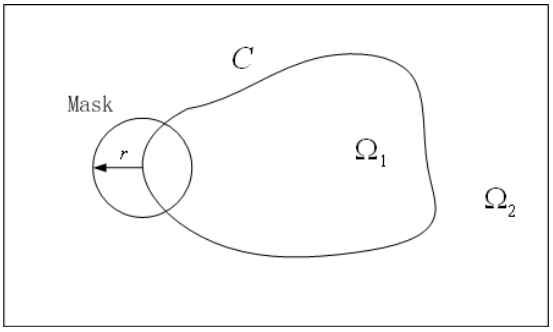

FIGURE 3. Mask of local region

where E_x^{local} is a weighted mean square error of the approximation of the image intensity $I(y)$ outside and inside the contour C, by the fitting values $f_1(x)$ and $f_2(x)$, respectively, with $M(x, y, r)$ as the mask assigned to the point x. And $f_1(x)$ and $f_2(x)$ are defined as follows:

$$\begin{cases} f_1(x) = mean(\{y \in \Omega_1\} \cap M(x, y, r)) \\ f_2(x) = mean(\{y \in \Omega_2\} \cap M(x, y, r)) \end{cases} \tag{8}$$

Therefore, the local energy function defined for the contour C is

$$E^{local}(C, f_1, f_2) = \int E_x^{local}(C, f_1(x), f_2(x))dx \tag{9}$$

We use the CV model's global energy

$$E^{global}(C, c_1, c_2) = \lambda_1 \int_{C_{in}} |I(x) - c_1|^2 \, dx + \lambda_2 \int_{C_{out}} |I(x) - c_2|^2 \, dx \tag{10}$$

Now, the energy function of global and local region-based active contour is defined as:

$$E^{GL}(C, f_1, f_2, c_1, c_2) = \omega E^{local}(C, f_1, f_2) + (1 - \omega) E^{global}(C, c_1, c_2) \tag{11}$$

where ω is positive constant ($0 \leq \omega \leq 1$). To handle topological changes, we will convert the energy function to a level set formulation in the next subsection.

3.2. **Level set formulation of the model.** In level set method, a contour $C \subset \Omega$ is represented by the zero level set of a Lipchitz function $\phi : \Omega \to \Re$, such that

$$\begin{cases} C = \{(x, y) \in \Omega : \phi(x, y) = 0\} \\ \Omega_1 = \{(x, y) \in \Omega : \phi(x, y) < 0\} \\ \Omega_2 = \{(x, y) \in \Omega : \phi(x, y) > 0\} \end{cases} \tag{12}$$

With the level set representation, the energy function in (9)-(11) can be written as below respectively:

$$\begin{aligned} E^{local}(\phi, f_1, f_2) = &\lambda_1 \int M(x, y, r) \, |I(y) - f_1|^2 \, H(\phi(x, y))dydx \\ &+ \lambda_2 \int M(x, y, r) \, |I(y) - f_2|^2 \, (1 - H(\phi(x, y)))dydx \end{aligned} \tag{13}$$

$$\begin{aligned} E^{global}(\phi, c_1, c_2) = &\lambda_3 \int |I(x) - c_1|^2 \, H(\phi(x, y))dx \\ &+ \lambda_4 \int |I(c) - c_2|^2 \, (1 - H(\phi(x, y)))dx \end{aligned} \tag{14}$$

$$E^{GL}(\phi, f_1, f_2, c_1, c_2) = \omega E^{local}(\phi, f_1, f_2) + (1 - \omega) E^{global}(\phi, c_1, c_2) \tag{15}$$

In practice, the Heaviside function H in the above energy functions is approximated by a smooth function H_ξ defined by

$$H_\xi(x) = \frac{1}{2} \left[1 + \frac{2}{\pi} \arctan\left(\frac{x}{\xi} \right) \right] \tag{16}$$

And the derivative of the proposed H_ξ is Dirac function

$$\delta_\xi(x) = H'_\xi(x) = \frac{1}{\pi} \left(\frac{s}{s^2 + \pi^2} \right) \tag{17}$$

In order to compute the level set function ϕ accurately, we need to regularize the level set function by penalizing its deviation from a signed distance function. As proposed in

[29], the level set regularization term is defined as

$$P(\phi) = \int \frac{1}{2}(|\nabla\phi(x)| - 1)^2 dx \tag{18}$$

In typical level set method of active contour, we need to regularize the zero level set by penalizing its length to derive a smooth contour during evolution. The function is defined as

$$K(\phi) = \int |\nabla H_\xi(\phi(x))|\, dx \tag{19}$$

Then, the entire energy functional in (15) is approximated by

$$F^{GL}(\phi, f_1, f_2, c_1, c_2) = E^{GL}(\phi, f_1, f_2, c_1, c_2) + \mu \mathrm{K}(\phi) + \upsilon \mathrm{P}(\phi) \tag{20}$$

where $\mu > 0$, $\upsilon > 0$ are constants as the weights of the term $\mathrm{K}(\phi)$ and $\mathrm{P}(\phi)$, respectively. This is the energy functional which will be used to find the object boundary of bovine iris.

For a fixed level set function ϕ, $F^{GL}(\phi, f_1, f_2, c_1, c_2)$ in (20) can be minimized with respect to the functions $f_1(x)$, $f_2(x)$, and constants c_1, c_2. By calculus of variations, it can be shown that the functions $f_1(x)$, $f_2(x)$ and constants c_1, c_2 that minimize $F^{GL}(\phi, f_1, f_2, c_1, c_2)$ satisfy the following Euler-Lagrange equations:

$$\int M(x, y, r)\, |I(y) - f_1|\, H(\phi(x, y))dy = 0 \tag{21}$$

$$\int M(x, y, r)\, |I(y) - f_2|\, (1 - H(\phi(x, y)))dy = 0 \tag{22}$$

$$\int |I(x) - c_1|\, H(\phi(x, y))dx = 0 \tag{23}$$

$$\int |I(x) - c_2|\, (1 - H(\phi(x, y)))dx = 0 \tag{24}$$

From Equations (21)-(24), we can get

$$f_1(x) = \frac{\int M(x, y, r) * H_\xi(\phi(x)) * I(y)dy}{\int M(x, y, r) * H_\xi(\phi(x))dy} \tag{25}$$

$$f_2(x) = \frac{\int M(x, y, r) * (1 - H_\xi(\phi(x))) * I(y)dy}{\int M(x, y, r) * (1 - H_\xi(\phi(x)))dy} \tag{26}$$

$$c_1 = \frac{\int H_\xi(\phi(x)) * I(x)dx}{\int H_\xi(\phi(x))dx} \tag{27}$$

$$c_2 = \frac{\int (1 - H_\xi(\phi(x))) * I(x)dx}{\int (1 - H_\xi(\phi(x)))dx} \tag{28}$$

To minimize the energy functional $F^{GL}(\phi, f_1, f_2, c_1, c_2)$ in (20) with respect to ϕ, we deduce the associated Euler-Lagrange equation for ϕ. Parameterizing the descent direction by an artificial time $t \geq 0$, the equation in $\phi(t, x, y)$ (with $\phi_0(x, y)$ defining the initial

contour) is

$$\begin{aligned}\frac{\partial \phi}{\partial t} &= \delta_\xi(\phi)\omega F^{local} + \delta_\xi(\phi)(1-\omega)F^{global} \\ &\quad + \mu\delta_\xi(\phi) div\left(\frac{\nabla\phi}{|\nabla\phi|}\right) + \upsilon\left(\nabla^2\phi - div\left(\frac{\nabla\phi}{|\nabla\phi|}\right)\right)\end{aligned} \tag{29}$$

$$\phi(0,x,y) = \phi_0(x,y) \text{ in } \Omega \tag{30}$$

$$\frac{\delta_\xi(\phi)}{|\nabla\phi|}\frac{\partial\phi}{\partial\vec{n}} = 0 \text{ on } \partial\Omega \tag{31}$$

where $\vec{n}$ denotes the exterior normal to the boundary $\partial\Omega$, and $\partial\phi/\partial\vec{n}$ denotes the normal derivative of ϕ, at the boundary. F^{local} and F^{global} are written as (32) and (33).

$$F^{local} = -\lambda_1 \int M(x,y,r)\left|I(y)-f_1\right|^2 dy + \lambda_2 \int M(x,y,r)\left|I(y)-f_2\right|^2 dy \tag{32}$$

$$F^{global} = -\lambda_3\left|I(x)-c_1\right|^2 + \lambda_4\left|I(x)-c_2\right|^2 \tag{33}$$

F^{local} and F^{global} represent the local intensity force and the global intensity force respectively. The two different forces influence the curve evolution complementary. In the region far away from the desired boundaries of object, where the intensity varies slowly, the values of f_1, f_2 got by local intensity information are almost the same, and the local force F^{local} is not capable to guide the contour toward the object boundaries. Therefore, the global force F^{global} dominates the curve evolution. In response, when the contour is near the object boundaries, the local force F^{local} dominates the curve evolution, which attracts the contour toward the object boundaries and provides the contour from passing the object boundaries.

4. **Implementation and Discussion.** Animal Iris Database (version 1.0) is adopted to evaluate the performance of the proposed method. The experiments are done in Matlab 7 on a PC with Intel Core 2 Duo 2.26GHz CPU, 2G bytes RAM, and Microsoft Windows XP Professional operating system. Furthermore, in order to measure the performance of the proposed method, Zhang's method [36] is also implemented on the same database and platform.

4.1. **Results.** Based on Equations (29)-(31), we use the finite difference method to discretize the level set function ϕ. The level set function ϕ is simply initialized as a binary step function which takes a negative constant value $-c_0$ for the inside region Ω_1 and a positive constant value c_0 for the outside region Ω_2. For the image Figure 4(a), we use the parameters $c_0 = 3$, $\lambda_1 = \lambda_2 = \lambda_3 = \lambda_4 = 1.0$, $\omega = 0.37$, $r = 5$, $\upsilon = 0.5$, time step $\Delta t = 0.1$, $\mu = 0.004 \times 255 \times 255$, and $\xi = 1.0$ for the Dirac function. The initialization contour is shown in Figure 4(b), noted that the original image is the same as Figure 2(b). And the inner and outer boundaries of bovine iris are shown in Figure 4(c) after 50 iterations. It is clearly that the proposed active contour model driven by global and local intensity information can handle the iris intensity inhomogeneity.

As shown in Figure 4(c), the inner boundary is a closed curve, and the outer boundary is not closed. Also the iris region in the image is shape irregularity, which is not conductive to the follow-up feature extraction. Here, we use a pair of concentric ellipses to approach the actual inner and outer boundary of iris, and then the iris is regularized into an elliptic ring. Furthermore, original image of bovine eye may contains eyelid and lash, which will influence the veracity of feature extraction. To eliminate the influence, the area $[-\pi/4, \pi/4]$ and $[3\pi/4, 5\pi/4]$ of the elliptic ring are selected to use, as the eyelid and lash usually appear in the area $[\pi/4, 3\pi/4]$ and $[5\pi/4, 7\pi/4]$. Then, the selected area will be

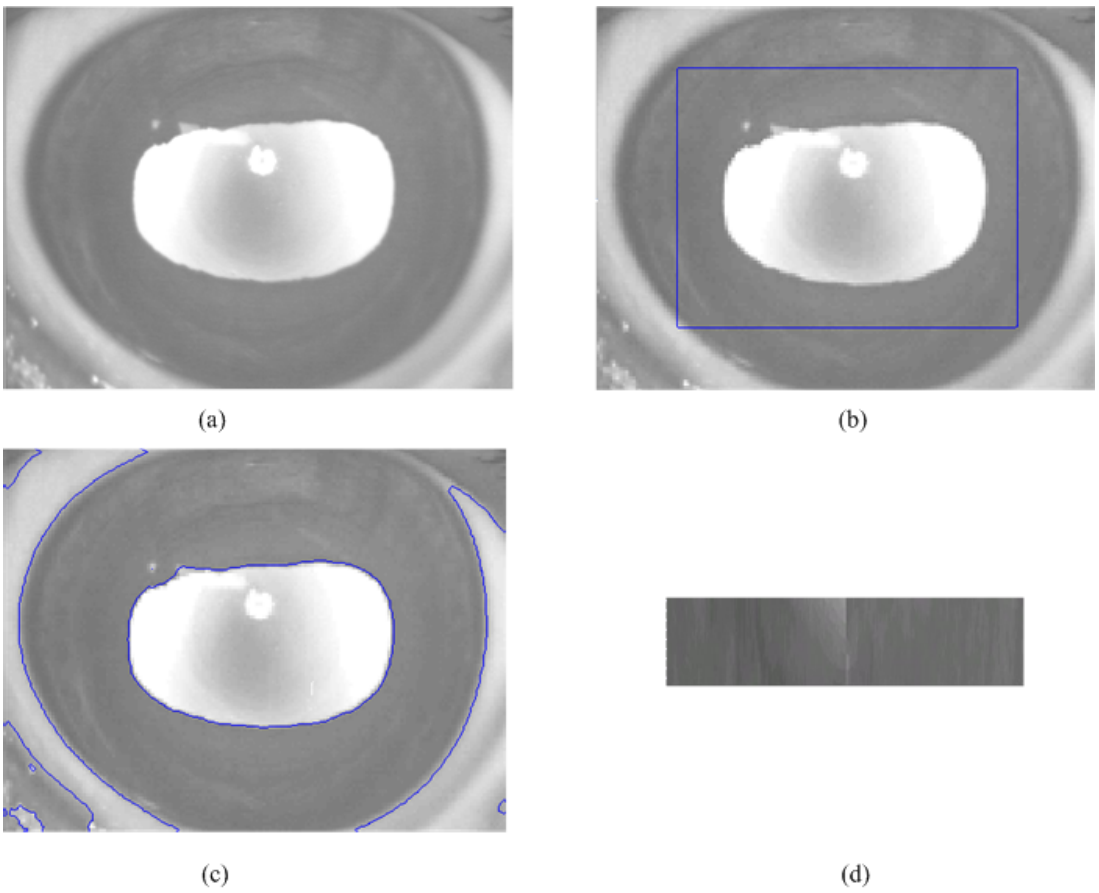

FIGURE 4. (a) Original image, (b) initialization contour, (c) segmentation result and (d) normalization result

transformed into a rectangle block by polar coordinate transformation. The normalization steps are listed as below.

Step 1: Find out the center point of the inner boundary, and this point is also considered as the center of the outer boundary.

Step 2: Get a pair of concentric ellipses, which cover the maximal numbers of inner and outer boundary points separately.

Step 3: Choose the interesting parts from the elliptic ring. Here the area $[-\pi/4, \pi/4]$ and $[3\pi/4, 5\pi/4]$ are selected.

Step 4: Reshape the selected parts into a rectangle with polar coordinate transformation.

Then, we get the normalized iris with above normalization steps from the original image as shown in Figure 4(d), which will be used in the following steps of iris recognition.

Two-dimension Gabor filters and Hamming distance are employed to test the performance of the proposed bovine iris segmentation method. Zhang's [36] two-step method is also implemented with the same feature extraction algorithm for a comparison. The experimental results are given in Table 1, from which we can see that the proposed method brings a significant improvement on the iris recognition performance, as the method obtains lower equal error rate (EER).

4.2. **Parameter analysis.** In the proposed model, $M(x, y, r)$ function uses the mean intensity to calculate the local energy, which is different from Gaussian kernel used in other global and local energy driven active contour models [30,31]. The radius r of the

TABLE 1. Performance of proposed method

	Equal Error Rate (EER)
Zhang's method [36]	2.23%
Proposed method	1.02%

ball selected by the $M(x, y, r)$ function is an important parameter to be considered when using the localized energies. Its size determines how much the localization information is used to segment the image. Hence, it should be chosen based on the scale of the objects of interest and the presence and proximity of the surrounding clutter. When attempting the capture objects that with nearby clutter, a small radius should be used. On the contrary, larger radius is useful when attempting to segment object with less nearby clutter. Therefore, in our experiment a small value $r = 5$ is used to get the boundary with nearby clutter.

The coefficients ω and $1-\omega$ are the weights of local and global energy respectively. The two positive parameters are used to govern the tradeoff between the local term and global term. The parameter ω should be set according to the intensity inhomogeneity presenting in the images. If the intensity homogeneity is not serious, the value ω is suggested to be equal to 0, which insures that the global force can dominate the curve evolution. Otherwise, ω should be given a larger value, which means the local force contributes to the curve evolution. In our experiment, $\omega = 0.37$ makes the local term contribute as an important part.

5. **Conclusions and Future Work.** In this work, we propose an improved Chan-Vese model for bovine iris segmentation, which is based on the techniques of curve evolution and level set theory. The energy function for the proposed model consists of global term, local term and regularization term. The iris image which is inhomogeneity can be efficiently segmented by incorporating the local image information into our model. Moreover, in order to the benefit of later feature extraction, ellipses are applied to shape and normalize the iris. Experiment on the real bovine iris images has demonstrated the desired segmentation performance of our proposed model.

Note that the weighting parameter of regularized term plays an important role [33]. In practice, tuning this parameter is not easy and may not be done automatically. Furthermore, for incorporating the local information, a ball with size r is applied in the proposed model. And the size of r depends on the scale of the objects of interest. Future work includes altering these parameters automatically which will allow the technique to be used with less tuning and interaction. Further extension can also be made to incorporate the shape information of bovine iris into the model.

Acknowledgment. The human iris image used in this paper is from the CASIA Iris Image Database (version 1.0), which is provided by Chinese Academy of Sciences – Institute of Automation, and the bovine iris image is from Animal Iris Database (version 1.0) provided by the Institute of Systems Engineering of Southeast University, Nanjing, China. This work is supported in part by the National Key Technology R&D Program of China during the 11th Five-Year Plan Period (No. 2006BAK02A16 and No. 2006BAK02A28), China Scholarship Council Postgraduate Scholarship Program, as well as by the Scientific Research Foundation of Graduate School of Southeast University (No. YBJJ1034). The authors also gratefully acknowledge the anonymous reviewers for their helpful comments and suggestions.

REFERENCES

[1] L. Flome and A. Safir, Iris recognition system, *US Patent 4641349*, 1987.
[2] J. Daugman, Recognizing people by their iris patterns, *Information Security Technology Report*, vol.3, no.1, pp.33-39, 1998.
[3] L. Ma, T. Tan, Y. Wang and D. Zhang, Local intensity variation analysis for iris recognition, *Pattern Recognition*, vol.37, no.6, pp.1287-1298, 2004.
[4] M. Suzaki, O. Yamakita et al., A horse identification system using biometrics, *Systems and Computers in Japan*, vol.32, no.14, pp.12-23, 2001.
[5] L. Zhao, S. Sun, Q. Kong and X. Wang, Food traceability system based on iris recognition middleware, *ICIC Express Letters*, vol.3, no.4(B), pp.1251-1256, 2009.
[6] J. Daugman, High confidence visual recognition of persons by a test of statistical independence, *IEEE Transactions on Pattern Analysis and Machine Intelligence*, vol.15, no.11, pp.1148-1161, 1993.
[7] J. Daugman, Demodulation by complex-valued wavelets for stochastic pattern recognition, *International Journal of Wavelets, Multiresolution, and Information Processing*, vol.1, no.1, pp.1-17, 2003.
[8] R. P. Wildes, Iris recognition: An emerging biometric technology, *Proc. of the IEEE*, vol.85, no.9, pp.1348-1363, 1997.
[9] L. Ma, Y. Wang and T. Tan, Iris recognition using circular symmetric filters, *Proc. of the 16th International Conf. on Pattern Recognition*, vol.2, pp.805-808, 2002.
[10] L. Ma, T. Tan and Y. Wang, Efficient iris recognition by characterizing key local variations, *IEEE Transactions on Image Processing*, vol.13, no.6, pp.739-750, 2004.
[11] J. Huang, L. Ma, Y. Wang and T. Tan, Iris model based on local orientation description, *Proc. of Asian Conf. on Computer Vision*, pp.954-959, 2004.
[12] S. Lim, K. Lee, O. Byenon and T. Kim, Efficient iris recognition through improvement of feature vector and classifier, *ETRI Journal*, vol.23, no.2, pp.61-70, 2001.
[13] X. Yuan and P. Shi, Iris feature extraction using 2-D phase congruency, *Proc. of the 3rd International Conf. on Information Technology Application*, Sydney, vol.33, pp.437-441, 2005.
[14] W. Boles and B. Boashash, A human identification technique using images of the iris and wavelet transform, *IEEE Transactions on Signal Processing*, vol.46, no.4, pp.1185-1188, 1998.
[15] V. Dorairaj, N. A. Schmid and G. Fahmy, Performance evaluation of iris based recognition system implementing PCA and ICA encoding techniques, *Proc. of SPIE Conf. on Biometric Technology for Human Identification II*, Orlando, vol.5779, pp.51-58, 2005.
[16] Z. He, T. Tan and Z. Sun, Iris localization via pulling and pushing, *Proc. of the 18th Conf. on Pattern Recognition*, Hongkong, vol.4, pp.366-369, 2006.
[17] A. Abhayankar and S. Schuckers, Active shape model for effective iris segmentation, *Proc. of SPIE Conf. on Biometric Technology for Human Identification III*, Orlando, vol.6202, pp.1-10, 2006.
[18] J. Daugman, New methods in iris recognition, *IEEE Transactions on Systems, Man, and Cybernetics-Part B: Cybernetics*, vol.37, no.5, pp.1167-1175, 2007.
[19] S. Shah and A. Ross, Iris segmentation using geodesic active contours, *IEEE Transactions on Information Forensics and Security*, vol.4, no.4, pp.824-836, 2009.
[20] K. Roy, P. Bhattacharya and C. Y. Suen, Recognition of unideal iris images using region-based contour model and game theory, *Proc. of IEEE the 17th International Conf. on Image Processing*, Hongkong, pp.1705-1708, 2010.
[21] M. Kass, A. Witkin and D. Terzopoulos, Snakes: Active contour models, *International Journal of Computer Vision*, vol.1, no.4, pp.312-331, 1988.
[22] V. Caselles, F. Catte, T. Coll and F. Dibos, A geometric model for active contour, *Numerical Mathematik*, vol.66, pp.1-31, 1993.
[23] V. Caselles, R. kimmel and G. Sapiro, Geodesic active contour, *International Journal of Computer Vision*, vol.22, no.1, pp.61-79, 1997.
[24] R. Malladi, J. A. Sethian and B. C. Vemuri, Shape modeling with front propagation: A level set approach, *IEEE Transactions on Pattern Analysis and Machine Intelligence*, vol.17, no.2, pp.158-175, 1995.
[25] C. Xu, A. Yezzi and J. L. Prince, On the relationship between parametric and geometric active contours, *Proc. of the 34th Asilomar Conf. on Signal, System, and Computers*, pp.483-489, 2000.
[26] T. Chan and A. Vese, Active contours without edges, *IEEE Transactions on Image Processing*, vol.10, no.2, pp.266-277, 2001.
[27] D. Mumford and J. Shah, Optimal approximation by piecewise smooth function and associated variational problems, *Communication on Pure and Applied Mathematics*, vol.42, pp.577-685, 1989.

[28] S. Lankton and A. Tannenbaum, Localizing region-based active contours, *IEEE Transactions on Image Processing*, vol.17, no.11, pp.2029-2039, 2008.

[29] C. Li, C. Xu, C. Gui and M. D. Fox, Level set evolution without re-initialization: A new variational formulation, *Proc. of IEEE Conf. on Computer Vision and Pattern Recognition*, vol.1, pp.430-436, 2005.

[30] L. Wang, C. Li, Q. Sun, D. Xia and C. Kao, Active contours driven by local and global intensity fitting energy with application to brain MR image segmentation, *Comput. Med. Imaging Graph.*, vol.33, no.7, pp.520-531, 2009.

[31] Y. Yu, C. Zhang, Y. Wei and X. Li, Active contour method combining local fitting energy and global fitting energy dynamically, *Proc. of International Conf. on Medical Biometrics*, pp.163-172, 2010.

[32] Y. Itai, H. Kim and S. Ishikawa, A segmentation method of lung areas by using snakes and automatic detection of abnormal shadow on the areas, *International Journal of Innovative Computing, Information and Control*, vol.3, no.2, pp.277-284, 2007.

[33] S. Yang and R. Radke, Level set segmentation with both shape and intensity priors, *IEEE the 12th International Conf. on Computer Vision*, pp.763-770, 2009.

[34] X. Zhang, Z. Sun and T. Tan, Texture removal for adaptive level set based iris segmentation, *Proc. of IEEE the 17th International Conf. on Image Processing*, pp.1729-1732, 2010.

[35] X. Wang, L. Zhao and Q. Kong, Iris recognition system design and development of large animals for tracing source of infection, *Proc. of the International Joint Conf. on Computational Sciences and Optimization*, vol.1, pp.610-613, 2009.

[36] M. Zhang, L. Zhao and X. Wang, An iris localization algorithm based on geometrical features of cow eyes, *Proc. of SPIE*, vol.7495, 2009.

[37] Z. Shi, L. Li, H. Wang, F. Wang, M. Zhao, Y. Wang and Q. Yao, Lung segmentation in chest radiographs using double localizing region-based active contours, *ICIC Express Letter, Part B: Applications*, vol.2, no.1, pp.69-74, 2011.